JOURNAL OF AIRCRAFT
Vol. 48, No. 2, March–April 2011

Failure Analysis of Cracks in the Upper Shaft of Torque Arm

Weiguo Hou,* Weifang Zhang, Qingyun Tang, Xiao Liu, Zongren Wang, and Meili Ding
Beijing University of Aeronautics and Astronautics, 100191 Beijing, People's Republic of China

DOI: 10.2514/1.C031169

In the periodic inspection of a plane having flown for 300 h, cracks were found in the upper shaft of the torque arm of the landing gear. In addition to visual examination, other experimental investigation techniques were 1) crack morphology and fracture characteristics by scanning electron microscopy, 2) metallographic observation of cracks, 3) chemical constituents and hydrogen-content testing, 4) hardness testing, 5) impact and bending simulation test, and 6) comparison of wear condition for the crack-free upper shafts with other batches. The results were obtained through the analysis of processing and experimental data. Because of higher surface frictional shear stress and tensile stress, the cracks propagated in the form of stress corrosion after the initiation, which was unrelated to the coating, matrix material, and hydrogen content.

I. Introduction

THE landing gear, as one of the main components of the plane, is a necessary support system of the plane for takeoff, landing, taxiing, moving, and parking on the ground. Since no direct transmission of torque exists between the inner rod and outer cylinder of the shock structure, the torque arm is used to transmit the torque by way of moment [1]. In every five planes having a 300 h periodic inspection, cracks were found in the upper shaft of the main landing gear torque arm, as shown in Fig. 1. The upper shaft is made of 30CrMnSiNi2A.

II. Experimental Procedure and Results

A. Observation of Crack Morphology

The morphology of crack area is shown in Fig. 2. Region I is the fracture of cracks with circumferential distribution formed. Many circumferential cracks were found to be parallel with the fracture on both sides, and circumferential frictional traces were found as well. In some areas the crack direction is consistent with the circumferential frictional traces, while in other areas a certain angle existed between them. Unlike the circumferential ploughing wear traces, it wore seriously in the 45° direction and obvious spallings could be found in some areas, as shown in Fig. 3. It can be judged that the surface of the upper shaft was subjected to higher torsion (shear stress) during the process of wearing.

B. Observation of Crack Fracture

Opened along the crack, the fracture can be obviously divided into four regions with different morphology (see Fig. 4). It contains the coating crack region (region I), quasi-cleavage fracture region (region II), intergranular fracture region (region III), and open-formation region (region IV). The surface of the crack belongs to the coating crack region, from which obvious radiation fracture can be found. As shown in Fig. 5, from the convergence direction of the radiation pattern, it can be observed that the crack was initiated from the coating surface and propagated into the matrix. The depth of regions I and II were measured to be 33 and 30–50 μm, respectively. Between the quasi-cleavage fracture region and the open-formation region was the intergranular fracture region (see Fig. 6), which took up a higher proportion (about 80%) of the fracture. The open-formation region was characterized by a thin dimple fracture (see Fig. 7) [2].

C. Metallographic Observation and Microstructure Analysis of Cracks

Many cracks were found when the crack area was sampled for metallographic observation (see Fig. 8). Some existed within the coating and did not propagate into the matrix, while others propagated into the matrix at different depths; the deeper one might be about 0.6–0.7 mm. The cracks in the matrix propagated along the crystal boundary and furcated at the local position (see Figs. 8 and 9). No decarbonizes and evident material defects were found. The metallurgical structure consisted of tempered martensite, lower bainite, and little residual austenite, with nothing abnormal detected.

D. Chemical Constituents and Hydrogen Content

The chemical constituents of the upper shafts 1–3 [3] are shown in Table 1. It can be concluded that the chemical structure meets the requirement. Table 2 shows the test results of hydrogen content of the upper shafts 1–3 [4].

E. Hardness Testing

The hardness of the coating and matrix for upper shafts 1–3 [3] shown in Table 3 meets the requirement.

F. Impact and Bending Simulation Test

Impact and three-point bending simulation were conducted, and the morphology of fractures is shown in Figs. 10 and 11. The coating fracture is characterized by brittle cracking, near which the matrix is

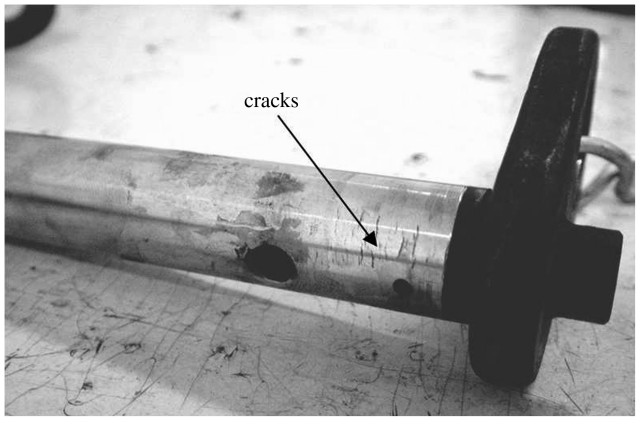

Fig. 1 Upper-shaft cracks.

Received 4 July 2010; revision received 29 October 2010; accepted for publication 29 October 2010.

*Ph.D. Candidate, School of Reliability and System Engineering; weiguohou@dse.buaa.edu.cn.

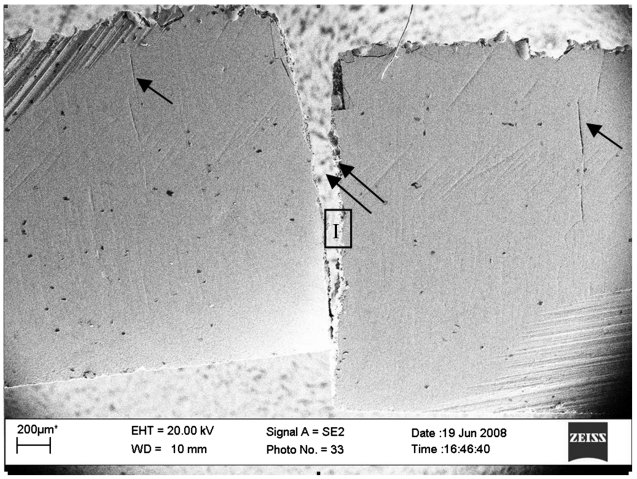

Fig. 2 Morphology of cracks.

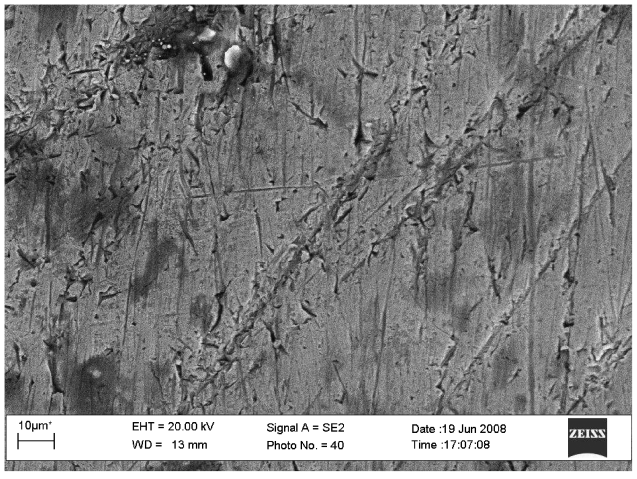

Fig. 3 Worn morphology at 45°.

the interconnection of quasi-cleavage and thin dimple. The fracture morphology of the local area near to the coating is intergranular (Fig. 11), and the extending area of the fracture morphology is equiaxed dimple (Fig. 10).

G. Observation of Wear Condition of the Crack-Free Upper Shafts

Wear conditions of the crack-free upper shaft's surface were observed, and they were from the same and other batches with equivalent-use time. The enlargement of worn morphology in the same batches is shown in Fig. 12), and other batches are shown in Fig. 13. It can be seen that circumferential and 45° tangential-direction wear scars appeared in both after a certain use time.

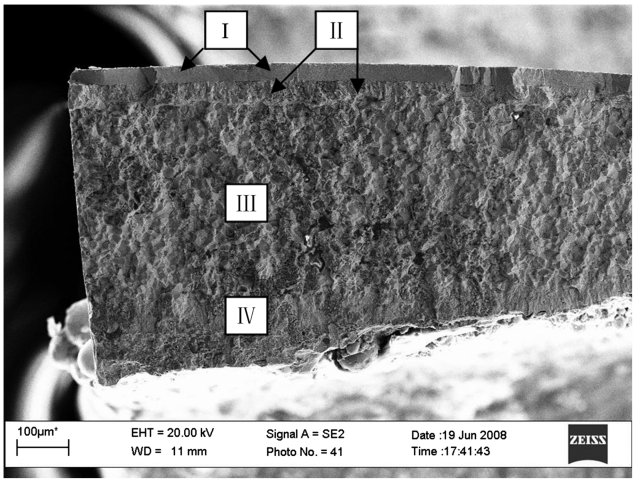

Fig. 4 Morphology of fracture.

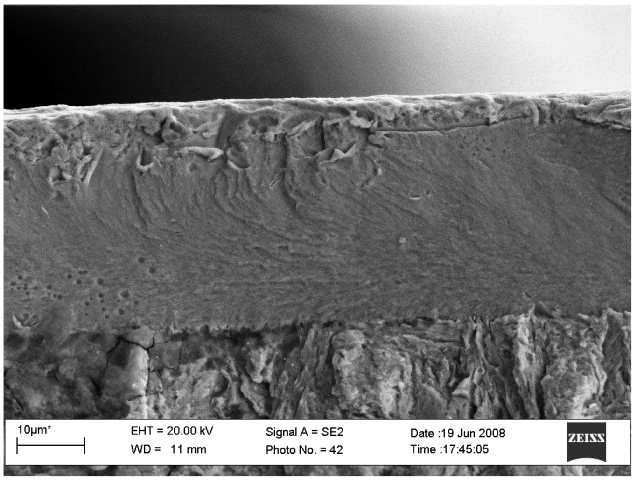

Fig. 5 Fracture morphology of the chromium coating.

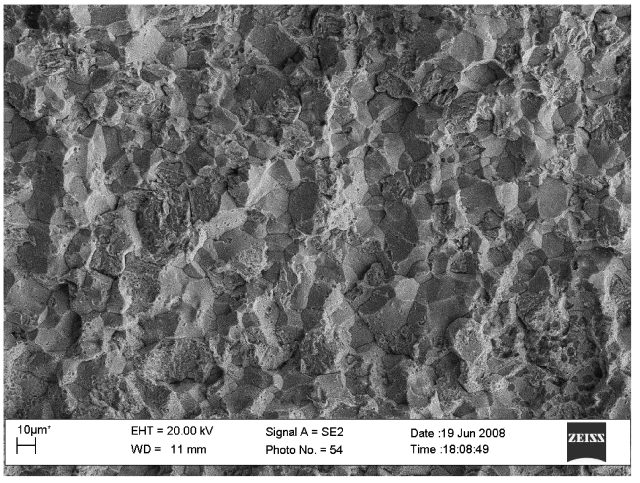

Fig. 6 Fracture morphology of the intergranular fracture region.

III. Analysis and Discussion

Through the observation and analysis of the metallurgical structure, there are no obvious changes found in the coating and matrix.

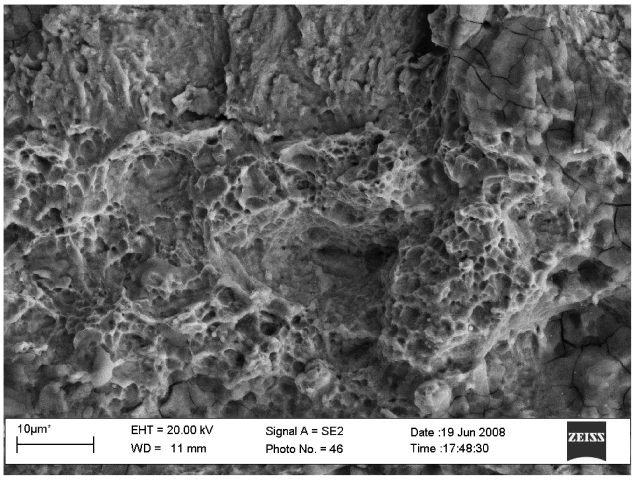

Fig. 7 Fracture morphology of the open-formation region.

Table 1 Test results of chemical constituents for weight percent

No.	C	Cr	Mn	Si	Ni	S	P
1	0.299	1.045	1.180	1.099	1.533	0.005	0.011
2	0.301	1.063	1.155	1.056	1.601	0.007	0.009
3	0.295	1.030	1.099	1.047	1.568	0.004	0.013
Standard	0.27–0.34	0.90–1.20	1.00–1.30	0.90–1.20	1.40–1.80	<0.015	<0.025

The hardness of the coating and matrix meets the requirements, which is demonstrated by the hardness testing. The fracture in the impact and bending simulation test is mainly characterized by a dimple crack. Intergranular fracture morphology may appear at the local area when the ultra-high-strength steel is slowly loaded, and a little intergranular character may also occur at the local area of fracture in bending test, related to its loading speed. These results indicate that the upper-shaft cracks have nothing to do with the material of the coating or matrix.

To enhance the capability of wearability and corrosion stability, the upper-shaft surface must be chrome-plated during the manufacturing process, in which the matrix probably absorbs hydrogen. If improper dehydrogenation process is conducted, hydrogen embrittlement will be prone to take place in service. There are no obvious microplasticity deformation traces, which commonly appear on the intergranular fracture by hydrogen embrittlement. Although microplasticity deformation trace does not appear sometimes under higher hydrogen content in the matrix, the hydrogen content of the upper shafts meets the requirements from the result of hydrogen content. In addition, the most important factor is that the hydrogen atoms diffuse to the areas of defect and high stress under the action of stress, in which cracks initiate, then spread around, with few cracks appearing, unlike the parallel cracks on the upper shaft's surface. Therefore, the cracks are unrelated to the hydrogen content.

There are some cracks that can be found in the surface of the upper shafts, the depths of which are different from each other. Some areas have superficial injury, with cracks only existing in the coating, while in other areas cracks propagate into the inner matrix, but the common feature of all the cracks is the large crack gap. It can be seen from the morphology of the fracture in which cracks initiate from the coating surface and propagate into the inner part through the interface of the coating and matrix.

Table 2 Test results of hydrogen content for upper shafts 1–3

No.	Hydrogen content, ppm
1	1
2	2
3	1

Table 3 Hardness-testing result of the upper shaft 2 (Vickers hardness H_V)

	Location				
	1	2	3	Mean value	Standard requirement
Coating	755	786	746	762	700–1000
Matrix	483	472	492	482 (HRC ≈ 48)	HRC > 41

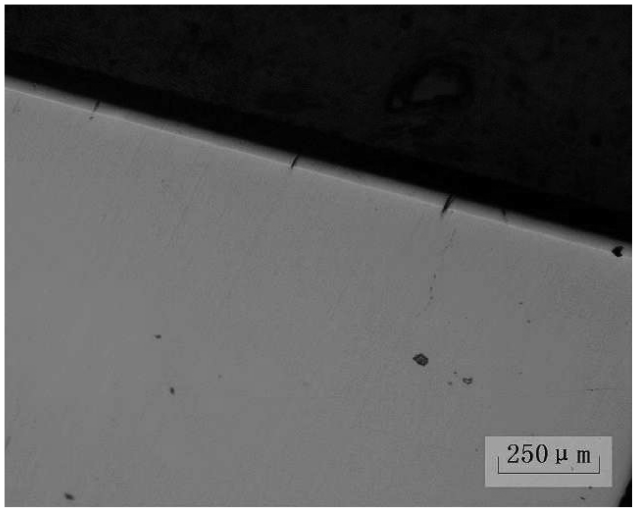

Fig. 8 Metallographic structure of cracks in coating area.

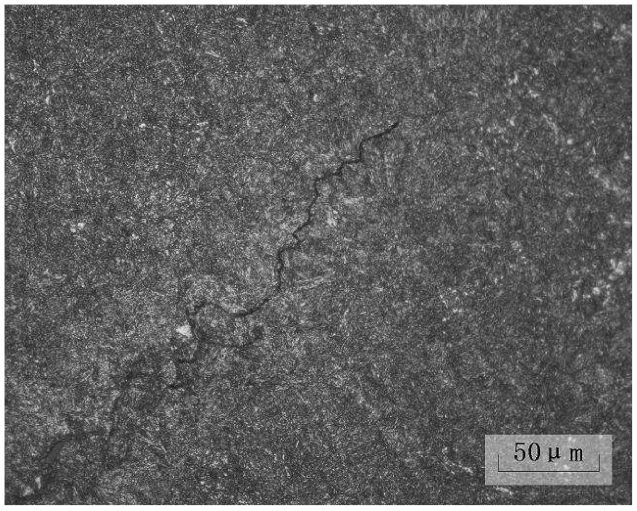

Fig. 9 Crack branching in the matrix.

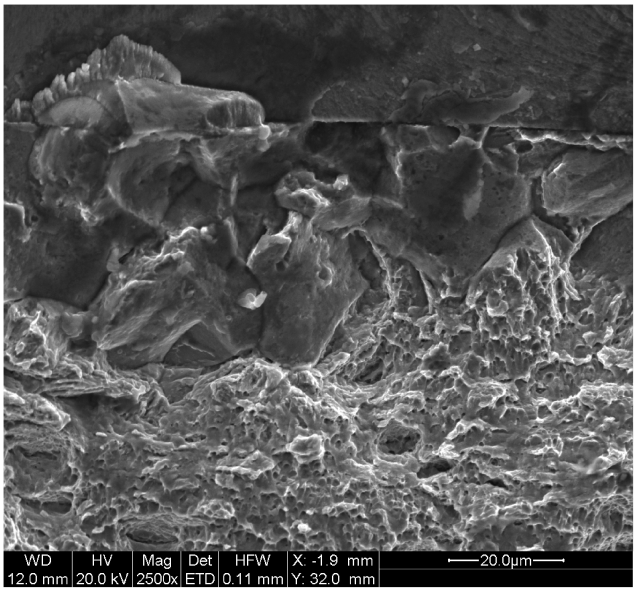

Fig. 10 Morphology of the coating brittleness fracture and nearby area of the bending sample.

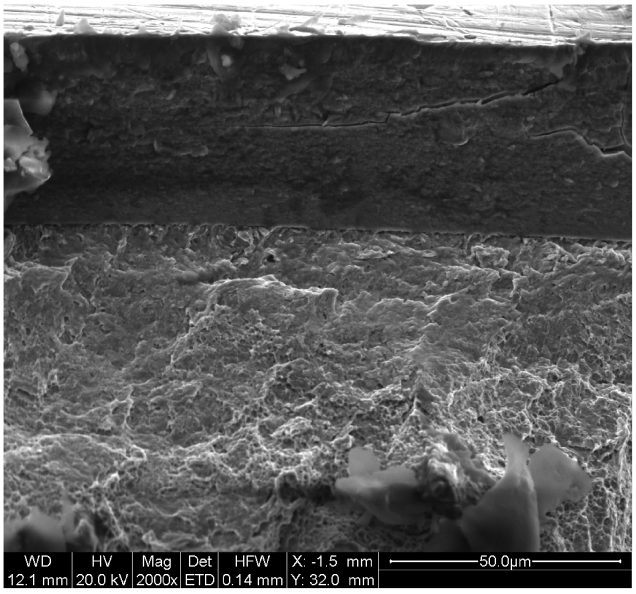

Fig. 11 Morphology of intergranular fracture nearby coating of the bending sample.

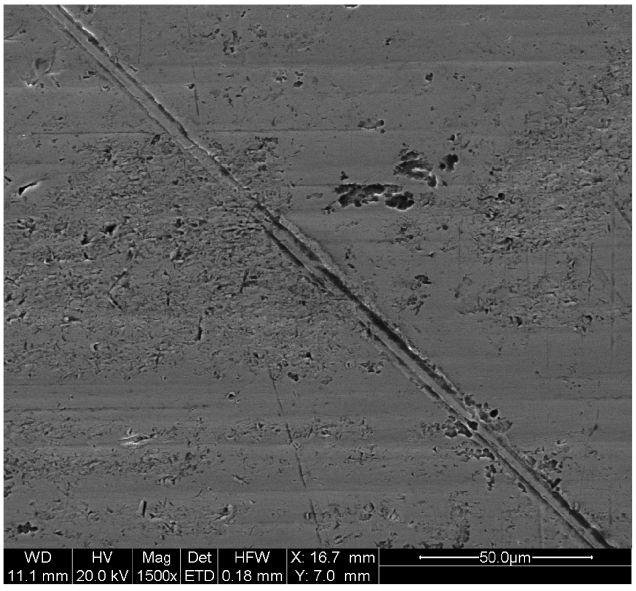

Fig. 12 Worn morphology of the same batch.

Judging from the assembly condition of the upper shafts, torsion bars, and pillar external tube lugs, the upper shaft is fixed, connected with the lugs by pins, and it can rotate in the copper bush if clearance fit exists (see Fig. 14) [1]. The AB part bears torsion stress when the upper-shaft lugs are forced by the steel rope. The cracks exist only in the AB part that bears torsion stress of the upper shaft. It can be seen from the cracks of the upper shaft and the surface wear condition that cracks are mainly circumferential and should be related to the torsion stress. An obvious abrasive wear in the furrow can be seen on the surface of the upper shafts, with or without cracks. The formation of the trace may have relation to the hard particles between the surfaces of the upper shaft and the copper bush, since there is no sealing that exists at either end of the bush. The hard particles scrape the surfaces when there is circumferential rotation between the upper shaft and the bush, creating some furrow wear traces. No high-contact friction shearing stress exists between the external surface of the upper shaft and the internal surface of the copper bush. Severe 45° tangential wear traces appear on the surface of the upper shaft with cracks, which are not caused only by the abrasive wear. Higher-friction shearing stress also exists on the surfaces of the upper shaft and the bush, contributing to the bad wear and even flaking.

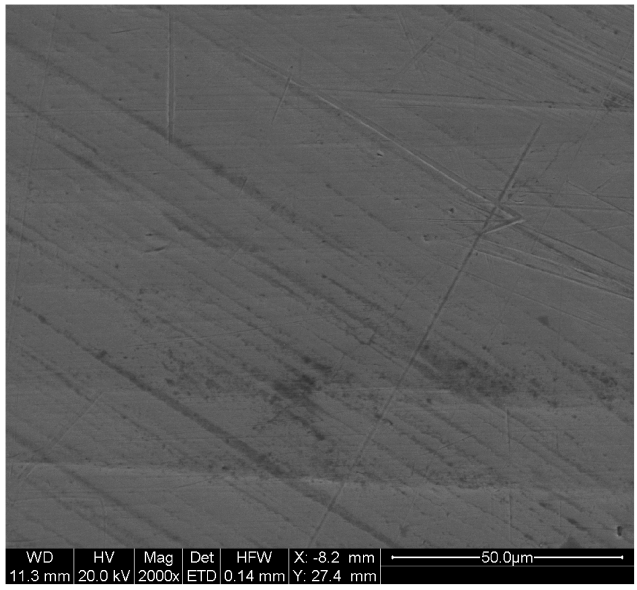

Fig. 13 Worn morphology of other batches.

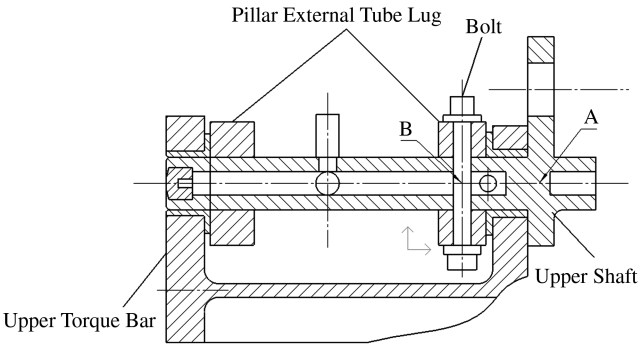

Fig. 14 Assembly of the upper shafts, torsion bars, and pillar external tube lugs.

The hard chromium-plating layers possess high hardness, good wearability, and anticorrosion capacity [1]. Because of the difference of their elastic modulus from the matrix material, the surface easily cracks, as the incoordination of deformation of the coating and matrix happens when the plating layers are loaded, especially with surface shear stress. From the morphology of the wear condition of the crack-free upper shafts, it is concluded that no evident wear morphology and spalling due to higher contact stress can be found, despite the abrasive wear in the furrow, which exists largely on the surfaces of the crack-free upper shafts in both the same and other batches. As a result, the formation of the upper-shaft surface crack should be related to the higher contact stress of contact surfaces. The superposition of tangent friction force and torsion stress caused by the contact stress leads to the crack of the upper-shaft coating.

The crack inside the coating propagates quickly, as the coating of the upper shaft is hard and brittle. In addition, the interface is well bonding for no crack or spalling between the coating and matrix. Higher gap stress concentration is generated after the coating crack, and it continues its quasi-cleavage propagation to a certain depth inside the matrix, at the instant of the coating crack. Without the anticorrosion protection of the coating as it cracks, the crack gets stress corrosion extension under lower stress.

IV. Conclusions

The hardness of the coating and matrix meets the requirement, and the formation of cracks is independent of the material of the coating and matrix and hydrogen content. The cracks propagate in the form

of stress corrosion after the initiation, due to higher surface frictional shear stress and torsional stress.

Acknowledgments

The authors gratefully appreciate the support by Hongdu Aviation Industry Group, Ltd., of China and also the language help from Zhang Wei, Tian Junwu, and Yao Jing.

References

[1] Li, Z., Zhang, Y., and Fang, W., *Vehicle Structure Theory*, Buaapress, Beijing, 2003, pp. 279, 293.

[2] Dong, Z., Zhong, P., Tao, C., and Lei, Z., *Failure Analysis*, National Defense Industry, Beijing, 2003, pp. 94, 149, 204.

[3] Davis, J. R., *Carbon and Alloy Steels*, ASM International, New York, 1996.

[4] Raymond, L., "Evaluation of Hydrogen Embrittlement," *Corrosion*, ASM Handbook, Vol. 13, ASM International, Materials Park, OH, 1987, pp. 283–284.